

Terahertz imaging for non-destructive evaluation of mural paintings

J.B. Jackson ^{a,*}, M. Mourou ^a, J.F. Whitaker ^a, I.N. Duling III ^b,
S.L. Williamson ^b, M. Menu ^c, G.A. Mourou ^d

^a Center for Ultrafast Optical Science, University of Michigan, Ann Arbor, MI, United States

^b Picometrix, Advanced Photonics, Inc., Ann Arbor, MI, United States

^c Center for Research and Restoration, The Louvre Museum, Paris, France

^d Laboratoire d'Optique Appliquée, ENSTA-Ecole Polytechnique, Paris, France

Received 3 July 2007; received in revised form 4 October 2007; accepted 11 October 2007

Abstract

The feasibility of applying time-domain, terahertz spectroscopic imaging to the evaluation of underdrawings and paint layers embedded within wall paintings is demonstrated. Metallic and dielectric paint patterns and a graphite drawing are resolved through both paint and plaster overlayers using a pulsed-terahertz reflectometer and imaging system. We calculated the bulk refractive indices of four common pigments and used them to confirm color domains in a terahertz-beam spectral image of a painting.

© 2007 Elsevier B.V. All rights reserved.

1. Introduction

Optical imaging and spectroscopy have become well-established tools in the evaluation and conservation of frescoes and other freestanding works of art. For instance, they are used in the analysis of the chemical composition of a wide variety of artist's media and they also find application in the identification of superficial changes, hidden layers of paint and sub-surface damage in art work. Raman [1], X-ray fluorescence [2], and near-infrared [3,4] spectroscopic techniques have been used for these purposes, along with ultraviolet (UV) fluorescence [2] and infrared (IR) [5,6] and microwave imaging [7]. In terms of conservation, it is ideal that the method of evaluation for historical artifacts such as frescoes and mural paintings – typically an inherent part of a building's infrastructure – be non-destructive, non-invasive, spatially precise, and applicable *in situ*. Although each of the aforementioned technologies may satisfy one or more of these requirements, in this paper we propose that the application of terahertz time-domain

spectroscopic imaging (THz-TDSI) [2,8] can satisfy all of them.

There exists two primary techniques of mural paintings. In the first, the artist applies pigments to a wet plaster surface – generally a combination of slaked lime (calcium hydroxide) and sand (silica). As the plaster dries, the calcium hydroxide reacts with carbonic acid in the air to produce calcium carbonate – which binds the pigments to the wall. In the second technique, an artist will paint on a dry wall of plaster, and use a binder such as egg or milk protein, to ensure that the pigments adhere to the wall. In both instances, thick layers of plaster – which may either obfuscate prior art or support the work on a new surface – are essential to understand the wall painting's creation as well as to serve in its repair.

While UV, Raman, and IR spectroscopic methods have all been used to study the surface layer of murals, none of them have the penetration depth to probe millimeter thick layers of plaster. X-rays and microwaves can penetrate thick layers, and are often used to find dislocations, water damage and other defects. However, X-rays have no depth resolution, and microwaves (at frequencies below tens of gigahertz) have poor lateral spatial resolution.

* Corresponding author. Tel.: +1 734 936 3849.
E-mail address: jbjz@umich.edu (J.B. Jackson).

In this work, the time delays and intensity signatures of terahertz pulses reflected from multilayer systems of plaster, painted surfaces and graphite sketches have been investigated in order to demonstrate the feasibility of using terahertz techniques for inspecting and resolving fresco artworks embedded in sub-surface layers within a wall or ceiling. We have observed that it is possible to identify hidden layers, including underdrawings (sketches) – through both coats of paint and freestanding tablets of plaster – and that one may deconstruct restored original frescoes so as to extract information on prior defects [9,10].

2. Experimental procedure

Terahertz time-domain spectroscopic imaging – currently used in quality-control, homeland-security, and medical-diagnostic applications – is a valuable tool because of the low energy and power of THz pulses [8]. In addition, most non-polar, non-metallic materials are relatively transparent to THz waves. Because the degree of reflection and absorption of such waves depends on the complex index of refraction of the dielectric, the technique is well suited for the characterization of most art supplies.

Here, data has been obtained on several fresco samples using two different pulsed-terahertz-beam schemes. The first, intended to establish the feasibility of time-domain ranging for layered media, employed a free-space, time-domain-terahertz reflectometer consisting of an interdigitated-metal-finger, semi-insulating-photoconductive-GaAs terahertz emitter and a low temperature-grown-GaAs (LT-GaAs) Hertzian-dipole receiver. These devices are photoexcited by a 100 fs-pulse-duration, mode-locked, Ti:Sapphire laser having a center wavelength at 810 nm and an 80 MHz repetition rate. The photoconductive (PC) emitter was pulsed-biased with a ± 5 V periodic square wave at 9.5 kHz fundamental frequency and synchronized with the lock-in amplifier measuring the receiver's pre-amplified photocurrent. The terahertz-beam has a 7° divergence angle emerging from the emitter, and therefore we collimate the beam using an 3" focal length high density polyethylene (HDPE) lens and then focus the beam (~ 4.5 mm FWHM) with a 6 in. focal length, 2 in. diameter gold parabolic mirror onto the sample fresco at a 45° incidence angle. A second gold parabolic mirror then re-collimates the reflected terahertz-beam onto the PC receiver. A single THz waveform (averaged between 64 and 128 times over 1–2 min acquisition time) was digitally acquired for every 1 mm horizontal step the fresco sample was translated across the beam focus.

The sample was composed of a 60 mm \times 35 mm \times 4.35 mm thick plaster-of-paris (calcium carbonate/calcium sulfate semihydrate/silica) slab. The dielectric paints were dry pigment compound powders – i.e., titanium dioxide (white), limonite iron oxide-based clay (burnt sienna), and mixed carbon-iron oxide (black) – bound to the dry plaster with water. The conductive paint was silver flake bound with a bisphenol resin. Fig. 1 shows the (a) front

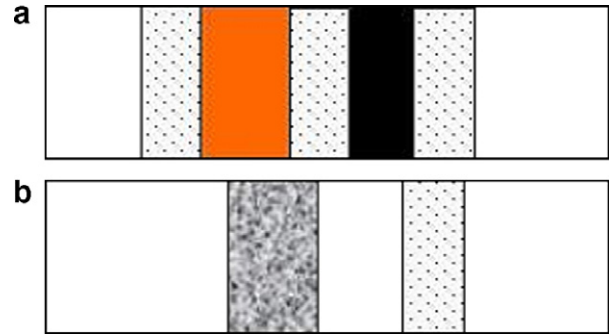


Fig. 1. (a) Front surface pattern, with strip widths: 5 mm white (dotted region); 8 mm burnt sienna; 5 mm white (dotted); 5 mm mixed black; 4.5 mm white paint. (b) Back surface pattern: 8 mm silver paint and 5 mm white paint, separated by a 6.5 mm unpainted region.

and (b) back one-dimensional (1-D) dielectric and metallic vertical stripe paint patterns, which were resolved through plaster and painted-plaster overlayers in this system by measuring the peak intensity of THz pulse reflections arising from refractive-index mismatches at the interfaces of different fresco layers.

In the second experiment, the integrated, optical-fiber-coupled transceiver head of a Picometrix T-RayTM terahertz-imaging system was scanned over the layered fresco samples, providing a normal THz-beam incident angle, a spatial resolution down to 2 mm, a selectable focal plane, and rapid data acquisition (< 5 min for a 7×7 cm plaster sample with 0.5 mm step size). In this experimental configuration, a two-dimensional (2-D) graphite sketch of a butterfly was first imaged through 4 mm of plaster-of-paris. The graphite sketch was then covered by a layer of opaque paint (pigment with water as binder) separated into four color quadrants: black, white, yellow ochre¹ (limonite iron oxide-hydroxide clay), and burnt sienna, as seen in Fig. 2.

3. Results

A typical set of time-domain data from a one-dimensional scan is shown in Fig. 3, where one observes independent pulsed-THz reflections from each side of a plaster substrate. The optical delay between the front and back surface reflections can be given by:

$$\Delta t = \frac{n_{pt}^2}{\sqrt{n_{pt}^2 - \sin^2 \theta}} \frac{d_{pt}}{c} + \frac{n_{pl}^2}{\sqrt{n_{pl}^2 - \sin^2 \theta}} \frac{d_{pl}}{c} \quad (1)$$

where n_{pt} , d_{pt} and n_{pl} , d_{pl} are the indices of refraction and thicknesses of the paint and plaster layers, respectively, θ is the incidence angle of the terahertz beam at the air/front surface interface, and c is the speed of light in a vacuum. The front-surface returns – their electric-field peaks influenced by bands of paint of the colors noted on the figure (e.g., to first order, the white paint stripes reflect a larger

¹ For interpretation of color in Fig. 2, the reader is referred to the web version of this article.

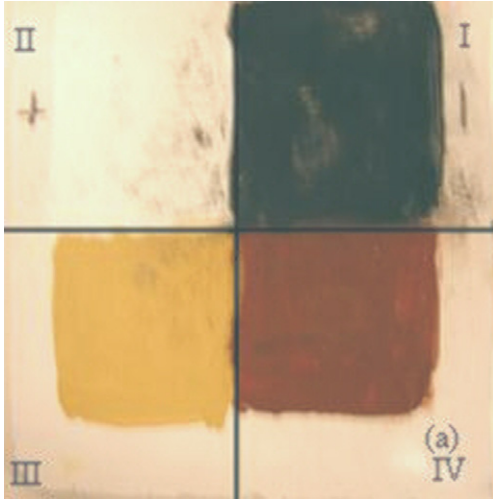


Fig. 2. Digital photograph of the painted surface of the butterfly sketch on plaster-of-paris.

peak signal than the other colors) – appear at the 7 ps time reference, while the back surface returns arrive about 55 ps later. As expected, it can be seen that the electrically-conductive-paint reflection is also out of phase with the returns from the dielectric white paint/plaster and plaster/air back interfaces residing behind the other front-surface paints.

Fig. 4 shows the integrated spectral power of the reflected electric field peak, given by

$$\int_{\Delta\nu} |F\{E(t)|_{t_a}^{t_b}\}|^2 d\nu \quad (2)$$

where the integrand is the Fourier transform of the time-domain electric field reflection in question with a single maximum peak between t_a and t_b picoseconds, and $\Delta\nu$ is the bandwidth of the incident terahertz pulse. On the front surface, the high contrast in reflectivity between the white, burnt sienna, and black paints easily distinguishes the color domains. The broadening of the measured color domains, as compared to their actual widths, may be attributed to a 6 mm $1/e$ THz spot size in this initial experiment. On the back surface – behind only the middle white and the burnt sienna paint stripes – the silver paint stripe yielded a significantly larger reflection than the white paint stripe – situated partially behind another white paint stripe (which significantly filtered the amount of field propagating through the plaster).

In the 2D scans, the pulsed-THz beams penetrated the 4 mm depth of a plaster substrate and, after time-gating the portion of the THz signal that returned solely from the rear of the substrate, a pattern of 1–2 mm wide graphite lines from the far side of the plaster was imaged. Specifically, the images of a butterfly are clearly observed when the THz-transceiver focal plane is adjusted to the back of the plaster substrate (Fig. 5). Images with air, wood, and additional plaster on the backside of the substrate were obtained, with the best contrast being seen with a plaster underlayer. While a variety of temporal windows around the discrete THz reflections were isolated, and different spectral ranges were selected from the FFTs acquired from these time-domain windows, multiple filtering stages have yet to be employed. Tighter focusing will also not only improve the spatial resolution, but it will also defocus

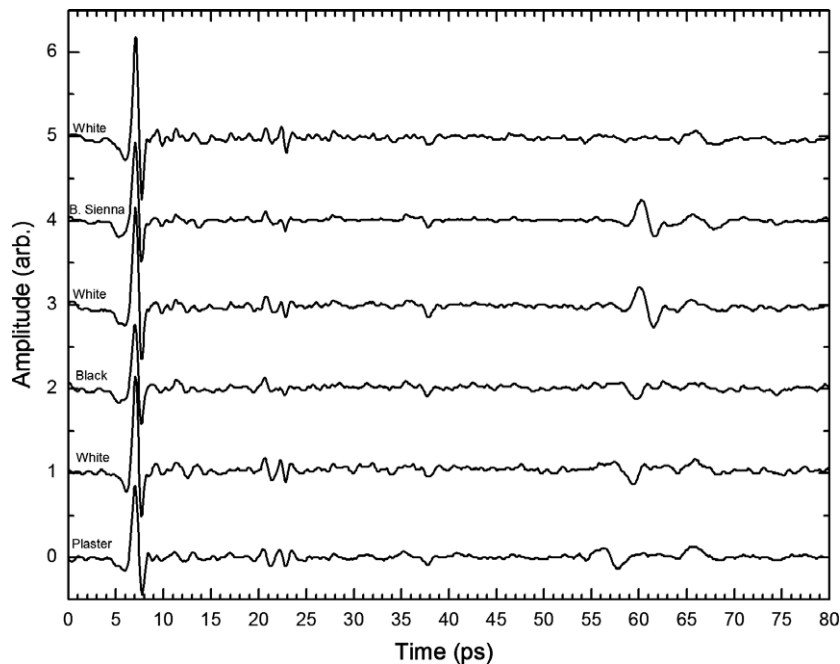


Fig. 3. Time-domain reflected THz pulses from six points along a line scan across the fresco painting depicted in Fig. 1. The waveform labels refer to the 1st surface, or front surface, pigment.

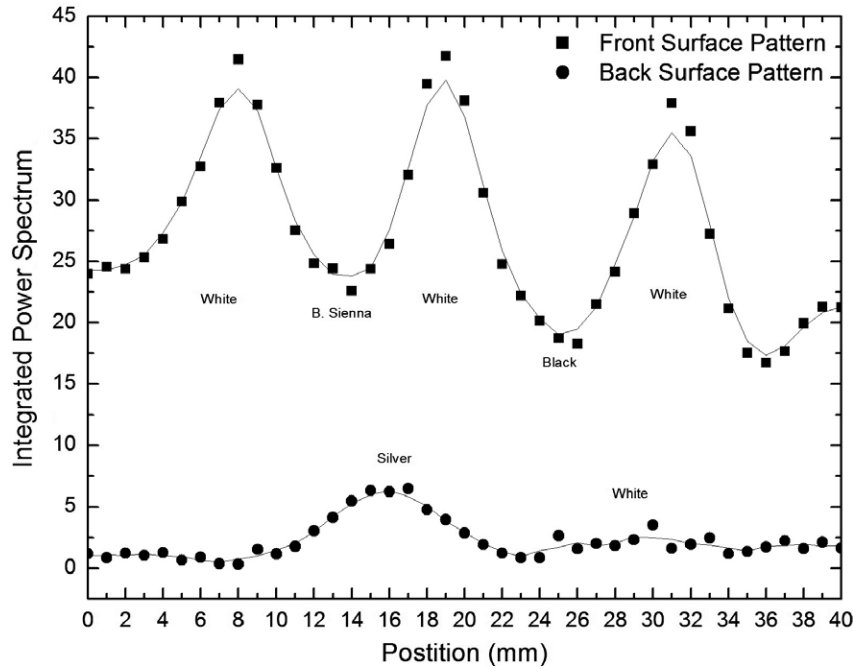


Fig. 4. Integrated power spectrum of front (square) and back (circle) surface reflections with solid-line smooth fit, measured in 1 mm increments across fresco painting.



Fig. 5. Time-domain power integration of THz-beam reflection from plaster/graphite/plaster interface. The graphite image of a butterfly, extracted from between plaster layers, is clearly recognizable.

layers that are not of interest and allow for better depth resolution.

Transmission THz-TDS measurements of the four pigments in densely packed optical cells were also performed. Comparing the time-domain transmission signals with and without the pigment samples present in their holders, absorption and phase delay due to the different pigments can be obtained, and thus complex refractive index values can also be determined and compared. Results from the

Table 1
Bulk index of refraction of dry pigments and plaster computed from time-domain-terahertz transmission measurements

Pigment	Quadrant	Bulk index
Black	I	1.57
White	II	1.70
Yellow ochre	III	1.35
Burnt sienna	IV	1.52
Plaster of paris		1.66

real part of the refractive index for the pigments and plaster are consolidated in Table 1.

The four pigments were also measured in reflection at normal incidence. They were applied wet to a cloth palette, then allowed to dry completely. Fig. 6 shows the pigments' spectral (a) reflected amplitudes and (b) reflectivities, respectively. Atmospheric water absorption lines can be seen at 0.56, 0.75, and 0.99 THz in Fig. 6a. At 0.66 and 0.89 THz, there appear to be absorption or loss features characteristic only of the cloth substrate. Note that the relative reflectivities are comparable to the relative indices of refraction for the pigments in Table 1. The similar slopes of the reflectivities for the black and burnt sienna pigments may be attributable to their iron-oxide composition.

Fig. 7 is a THz image of the graphite butterfly sketch emerging from under the four quadrants of paint layers from Fig. 2. The gray scale corresponds to the integrated spectral power between 0.14 and 0.48 THz. This range was selected to optimize the contrast between each color, based on the reflectivities given in Fig. 6b. The white pigment has the greatest reflectivity and appears light in the image, whereas the yellow ochre pigment appears darkest

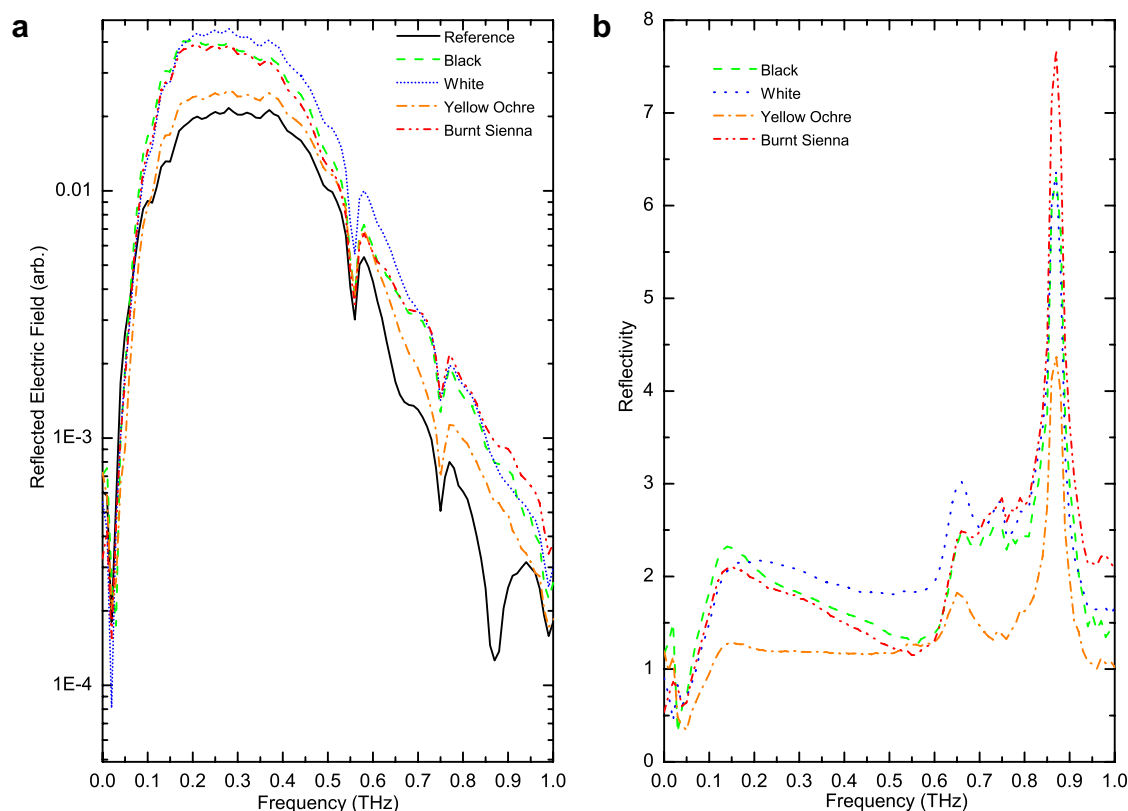


Fig. 6. Electric-field (a) amplitude and (b) reflectivity spectra of black, white, yellow ochre and burnt sienna pigments obtained via TD-THz reflection measurement. (For interpretation of the references to colour in this figure legend, the reader is referred to the web version of this article.)

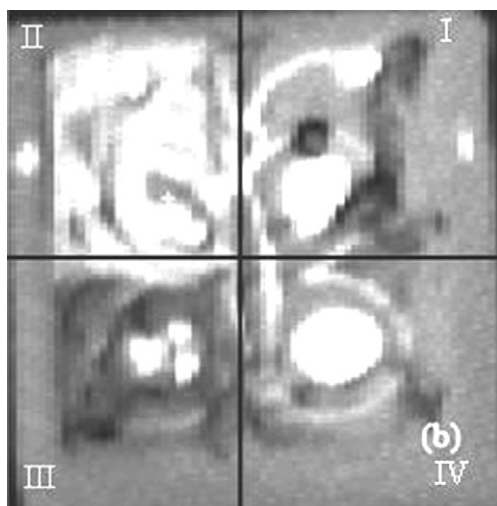


Fig. 7. THz-TDS image of the painting, with the sub-surface butterfly underdrawing visible through the surface. The image was formed using a power integration of the spectral information between 0.14 and 0.48 THz.

due to its low reflectivity. The black and burnt sienna pigments are indistinguishable from each other in this trial. Changes in the thickness and composition of the paint layers are also discernible. For spectral bands above 0.6 THz, the white and yellow ochre paint layers appear opaque, though the underdrawing can still be seen through the black and burnt sienna layers.

4. Conclusions

The ability to isolate interface reflections propagating through optically dense or opaque media, as well as the ability to distinguish reflections from different color domains demonstrates that Terahertz ranging and imaging have great potential for analysis of mural paintings in a completely non-invasive manner. Further investigation, including a spectroscopic study of pigments, plasters and other artistic media, will provide art historians and conservators with a dramatic improvement in investigative techniques.

Acknowledgement

The authors would like to thank Jeff White at Picometrix for his guidance with instrumentation.

References

- [1] G. Burrasato, M. Calabrese, A.M. Gueli, S.O. Troja, A. Zicarelli, J. Raman Spectrosc. 56 (2004) 879.
- [2] W. Köhler, M. Panzer, U. Klotzsch, S. Winner, M. Helm, F. Rutz, C. Jördens, M. Koch, H. Leitner, Non-destructive investigation of paintings with THz-radiation, in: European Conference of Non-Destructive Testing 2006 Proceedings, 2006, Poster 181.
- [3] D. Barilaro, V. Crupi, D. Majolio, G. Barone, R. Ponterio, J. Appl. Phys. 97 (2005) 044907.

- [4] S. Bruni, F. Cariati, L. Consolandi, A. Galli, V. Guglielmi, N. Ludwig, M. Milazzo, *Appl. Spectrosc.* 56 (2002) 827.
- [5] A. Casini, F. Lotti, M. Picollo, L. Stefani, E. Buzzegoli, *Stud. Conserv.* 44 (1999) 39.
- [6] Underdrawings in Renaissance paintings, *Art in the Making*, National Gallery Company Limited, London, GB, 2002.
- [7] M. Pieraccini, D. Mecatti, G. Luzi, M. Seracini, G. Pinelli, C. Atzeni, *NDT&E Int.* 28 (2005) 151.
- [8] D. Mittleman, M. Gupta, R. Neelamani, R.G. Baraniuk, J.V. Rudd, M. Koch, *Appl. Phys. B: Laser Opt.* 68 (1999) 1085.
- [9] S. Baronti, A. Casini, F. Lotti, S. Porcinai, *Appl. Opt.* 37 (1998) 1299.
- [10] Y. Watanabe, K. Kawase, T. Ikari, H. Ito, Y. Ishikawa, H. Minamide, *Appl. Phys. Lett.* 83 (2003) 800.